

Color stability and pH-indicator ability of curcumin, anthocyanin and betanin containing colorants under different storage conditions for intelligent packaging development

Alaitz Etxabide^{abc*}, Paul A. Kilmartin^c, Juan I. Maté^{ab}

^aALITEC Research Group, Department of Agronomy, Biotechnology and Food, School of Agricultural Engineering, Public University of Navarre (upna/nup), 31006 Pamplona-Iruña, Spain.

^bResearch Institute for Innovation & Sustainable Development in Food Chain, Department of Agronomy, Biotechnology and Food, Public University of Navarre (upna/nup), 31006 Pamplona-Iruña, Spain.

^cSchool of Chemical Sciences, The University of Auckland, Private Bag 92019, Auckland, New Zealand.

*Corresponding author

Alaitz Etxabide

Public University of Navarre (upna/nup)

School of Agricultural Engineering

Department of Agronomy, Biotechnology and Food

Campus Arrosadia s/n

Edificio los Olivos

31006 Pamplona-Iruña (Spain)

E-mail: alaitz.etxabide@unavarra.es

Telephone number: +34 948 16 9139

ABSTRACT

8.8 MT of food wastes are annually generated in the EU, in part due to the lack of real-time food freshness information provided by current food data labels. To address this issue, intelligent packaging strategies are being developed. In this study, in search of new natural and food grade pH-indicators, color stability and variability of curcumin (E-100), betanin (E-162), and anthocyanin (E-163) containing food colorants were studied in solution under different food storage conditions and pHs by light absorbance, color, pH and turbidity measurements. E-100 provided color variations (yellow/brown-yellow) at pH>9 and was particularly photosensitive since a color loss of 67% was observed after 1 day of storage. E-162 and E-163 colorants, however, were thermosensitive and showed significant lower loss of color (30%) after 28 days of storage. E-163, especially, presented a broader color response (red-purple-blue-green) over a wider pH range. Furthermore, color variations at different pHs were dependent upon colorant type and concentration.

KEYWORDS: Curcumin, anthocyanin, betanin, natural colorants, color stability, pH indicator.

1. INTRODUCTION

One third (about 1.3 billion tons) of food produced for human consumption is lost or wasted in the food supply chain every year. Focusing on developed countries, more than 40% of food losses happens at retail and consumer levels, due to legal requirements regarding food quality or safety, as well as consumers' expectations and decision-making criteria (FAO, 2015).

When it comes to consumers' judgement, food date labelling influences the decision of many customers at the point of food consumption, especially close to or past the date on the label. This makes data label a significant contributor to creating unnecessary food waste, especially at the household level (Raak et al., 2017; Wilson et al., 2017). In fact, up to 10% of the 88 million tons of food waste generated annually in the EU are linked to date labelling (European Commission, 2018), since data labels such as "Best Before" refers to quality issues distant to food safety ones. This means that the products are safe to eat and do not have to be discarded after the date, as long as they are properly stored (FDA, 2019). Consequently, great amounts of edible, safe, tasteful, and nutritious food products are unnecessarily disposed of. Given that current date labels do not provide consumers with real-time information about food freshness, safety, and quality, it is evident that there is an urgent need to replace or supplement food date labels for more accurate food control.

Intelligent packaging is an emerging area of food technology which is attracting a lot of attention in the food industry. Such systems contain components that monitor the condition of packaged food or its environment, to provide the consumer with correct information about the conditions of the product and the surrounded environment during transport and storage (European Commission, 2009). To this end, temperature, humidity, pH change, and gas-level (O_2 and CO_2) indicators are used as integral part of the package or as separate components placed inside the package (Fang et al., 2017; Won et al., 2016; Yam, 2012; Yousefi et al., 2019). Among them, pH-indicators can be suitable indicators for intelligent packaging system development (Kang et al.,

2018; Zhai et al., 2018), since pH changes occur with the spoilage of many food products. Considering consumer preference for the use of natural products over synthetic chemicals, and that way in which colorants may come in contact with foodstuffs, the search for natural and food grade pH-indicators is of utmost importance for the development of food intelligent packaging systems.

In this context, natural food colorants extracted from plants and root crops, such as curcumin, betanin, anthocyanin and chlorophyll, have shown color sensitivity to pH which makes them suitable indicators for intelligent packaging system development (Chen et al., 2020; Qin et al., 2020). However, given that the physicochemical stability of natural colorants is affected by many factors including pH, light, temperature, and presence of water (West & Mauer, 2013), the use of natural colorants as pH-indicators requires a detailed knowledge of their stability against possible degradation processes, especially at the point of sale. It is also necessary to know the conditions that control these alterations in order to prevent such variations by taking effective strategies and so, ensure sufficient stability of the colorants to act as effective pH-indicators.

The main purpose of this work was to search for suitable natural and food grade colorants to be used as pH-indicators for the development of intelligent packaging. In this work, curcumin, betanin and anthocyanin containing natural and food grade colorants were studied prior to their use as pH-indicators in intelligent food packaging systems, in order to analyze their suitability as pH-indicators and, if needed, propose some possible solutions to ensure their stability. The stability of colorants was analyzed in solution and under different commercial food storage conditions. In addition, the effect of colorant concentration on color change by pH modification was investigated. Changes in colorant solutions were assessed through color, light absorbance capacity, thermo-gravimetric analysis, pH, and turbidity characterizations.

2. MATERIALS AND METHODS

2.1. Materials

Natural and food grade colorants were kindly supply by Chr Hansen: T-PT8-WS is a dark yellow to brown viscous liquid produced by the extraction of pigments from turmeric root (*Curcuma longa* L.), with curcumin as the major coloring principle and polysorbate 80 present as a non-ionic emulsifier (Chr. Hansen Natural Colors A/S, Denmark); B-50-WS is a dark purple liquid produced by the extraction of pigments from red beet (*Beta vulgaris* L.) and its subsequent pasteurization, with betanin the major coloring principle and citric acid the acidity regulator (Chr. Hansen Natural Colors A/S, Denmark); ColorFruit Carrot 9 WS is a dark red liquid, produced by the extraction of pigments from black carrots (*Dacus carota* L.) and its subsequent pasteurization, with anthocyanins as the major coloring principle and citric acid the acidity regulator (Chr. Hansen Italia SpA, Italy). All colorants were water soluble. In the European Union, curcumin, betanin, and anthocyanin containing colorants are categorized under classification number E-100, E-162 and E-163, respectively (Commission Regulation, 2011), so same numbers have been used to label the colorants in this study. NaOH (1 M) and HCl (1 M) (Panreac, Barcelona, Spain) were used to prepare lower normality basic/acid solutions by diluting in distilled water.

2.2. Calibration curves

Calibration curves for the colorants were obtained by UV–Vis spectroscopy (ThermoFisher, Barcelona, Spain). 4 mL of diluted samples in distilled water were prepared and the wavelengths of maximum absorbance (λ_{\max}) for E-100, E-162 and E-163 were measured (424, 532, 526 nm, respectively). Standard solutions of the colorants were then prepared over certain concentration ranges (0.01-0.09 mg/mL, 0.25-1.70 mg/mL, 0.25-1.70 mg/mL) to establish calibration curves for E-100 ($y = -0.03521 + 12.112x$, $R^2 = 0.999$), E-162 ($y = 0.04189 + 0.55343x$, $R^2 = 0.997$) and E-163 ($y = -0.03681 + 0.62588x$, $R^2 = 0.998$), respectively, at each colorant λ_{\max} . These calibration curves were used to prepare samples with the same absorbance values (same color intensity) at each colorant λ_{\max} .

2.3. Colorants stability assessment at different storage conditions

2.3.1. Preparation of samples and storage

As the stability of natural compounds usually decreases faster in presence of higher amounts of water (West & Mauer, 2013), the colorants were analyzed in solution. Samples were prepared by dissolving the required amount of the colorants in distilled water, so that the resulting dissolutions presented absorbance values of 1 and thus the same color intensity. 1500 mL of solution was prepared for each replicate (n=3) of each colorant, and then glass transparent bottles (60 mL) were filled with 50 mL of colorant solution, closed by screw caps and stored horizontally without a predefined order in temperature and light controlled chambers (Tarre SA, Pamplona-Iruña, Spain) at four different storage conditions: i) 4 °C in the dark (T4NL); ii) 4 °C in cycles of light-darkness of 16:8 h (T4L) and 1007 ± 81 Lux of average luminous intensity (Sylvania T8 Luxline Plus F36W/840, 4000 K - Cool White color temperature); iii) 22 °C in the dark (T22NL) and; iv) 22 °C in cycles of light-darkness of 16:8 h (T22L) and 976 ± 71 Lux of average luminous intensity. T4L and T22L storage conditions were selected in order to simulate chilled and ambient commercial food storage conditions, respectively, of a local supermarket (E.Leclerc, Pamplona-Iruña, Spain). A sample for each replicate, colorant and storage condition was randomly taken at specific time points (0, 1, 3, 5, 7, 14 and 28 days) to analyze the stability (color, light absorbance capacity, pH and turbidity) over time. Analyzed samples were discarded after characterization.

Illuminance measurements were carried out by placing a multimeter ALMEMO® 2290-4 V5 with a Lux probe head (type FLA613VL) inside the chambers under T4L and T22L storage conditions. Measurements were randomly taken on weekdays and in light cycles during storage.

2.3.2. Color measurements

Visual color was measured using a DigiEye colorimeter (VeriVide, Leicester, UK), which consisted of a lighted cabinet, a calibrated Nikon digital photo camera and DigiEye v.280 software. The

measurements were performed under the standard CIE illuminant D65, which represents natural daylight with a correlated color temperature of 6500 K. For that, 4 mL of a sample was poured into a plastic PS cuvette which was then placed in the middle of the cabinet. An image of the sample was captured by the photo camera and analyzed using the software. Color measurements (L^* , a^* and b^*) were recorded against a selection of standard illuminants for the selected area of the image using the DigiPix tool. The selected area was defined using a rectangle area which covered one fifth of the filled part of the cuvette's image. Five areas of the image were analyzed for each replicate ($n=3$), colorant, storage condition and time.

2.3.3. Color intensity measurements

Color intensity was measured by MultiSkan GO UV-vis spectroscopy (Thermo Scientific, Madrid, Spain). For that, 400 μL of a sample was placed in a 96 microwell plate (Thermo Scientific, Madrid, Spain) and the light absorption of each replicate ($n=3$), colorant, storage condition and time was measured from 300 to 800 nm.

2.3.4. Thermo-gravimetric analysis (TGA)

Thermo-gravimetric measurements were performed in a TA instruments (Q5000 V3.17 Build 265, New Castle, USA). The raw food colorants were first frozen and freeze-dried before their thermal stability was tested from 25 °C up to 600 °C at a heating rate of 10 °C/min under air flow (50 mL/min) to induce thermo-oxidative reactions (simulate the real degradation process).

2.3.5. pH measurements

pH of the solutions was measured by a pH FiveEasy™ pH meter (Mettler Toledo, Barcelona, Spain), after performing a 3-point calibration. One measurement was taken for each replicate ($n=3$), colorant, storage condition and time.

2.3.6. Turbidity measurements

The turbidity was measured using a Hach model 2100 turbidimeter (Barcelona, Spain). 30 mL of a solution was poured into the turbidimeter sample cell which was equilibrated for 5 s before

each measurement. Turbidity values were calculated as an average of three measurements for each replicate (n=3), colorant, storage condition and time.

2.3.7. Antimicrobial activity of colorants

The antimicrobial activity of the colorants as a function of concentration was evaluated using the minimum bactericidal concentration (MBC) assay. Inocula of *E. coli* and *S. aureus* were first cultured in TSB broth at 37 °C under constant shaking of 200 rpm overnight. 8% w/v food colorants samples in TSB broth were then prepared and 100 µL of the homogenized colorant solutions was dispensed into the first row of wells of the 96-well plate (n=3) and serially diluted across the plate containing 50 µL of TBS medium base by a dilution factor of two were carried out. Broth containing microbial suspension alone was used as positive control. To all wells, microbial suspension with a concentration of 10⁶ CFU/mL (50 µL) was added so that the final colorant concentrations were 4, 2, 1, 0.5, 0.25, 0.125, 0.065 and 0 % w/v. The 96-well plates were then incubated at 37 °C under constant shaking of 200 rpm overnight. 20 µL of each well was then plated out in triplicate onto TSB-Agar plates and incubated at 37 °C overnight. The MBC endpoint was defined as the lowest concentration of antimicrobial agent that kills >99.9% of the initial bacterial population.

2.4. Effect of colorant concentration and pH on color variation

Samples were prepared by dissolving the required amount of colorants in distilled water so that the resulting solutions presented absorbance values of 0.25, 0.50 and 1.00. To this end, 100 mL of solution was prepared for each replicate (n=3) of each concentration and colorant, and then glass transparent bottles (12 mL) were filled with 6 mL of each solution. Solutions of NaOH and HCl of different normality were used as pH modifiers. 100 µL of a pH modifier was added to a sample in order to examine the effect of an external stimuli on the sample's color properties with a minimal modification to the initial solution concentration. Afterwards, the glass containers were close by screw caps and stored without a predefined order in a temperature and light controlled chamber at the most severe storage condition (T22L) for one day. The effect

of pH modifiers addition on different colorant concentration solutions was analyzed by measuring sample color and UV-vis absorbance before and after storage.

2.5. Color reversibility

For each colorant, samples with absorbance values of 0.25, 0.50 and 1.00 were prepared (n=3), and then glass transparent bottles (12 mL) were filled with 6 mL of each colorant solution. After that, 100 μ L of 0.5 M NaOH, 0.5 M HCl, 1.0 M NaOH and 1.0 M HCl were added within 1 minute intervals, and finally, 1.0 M NaOH was added before samples were stored at T22L conditions. A photo of the glass container with the colorant was taken using DigiEye every time the pH of the colorant solution was modified.

2.6. Statistical analysis

Data were subjected to one-way analysis of variant (ANOVA) by means of an SPSS computer program (SPSS Statistic 25.0). Post hoc multiple comparisons were determined by the Tukey's test with the level of significance set at $P < 0.05$.

3. RESULTS AND DISCUSSION

Calibration curves showed that E-100 was a more powerful colorant than E-162 and E-163 since much lower concentrations (almost 20 times less) were required to obtain the same absorbance values (color intensity) of the colorants in solutions.

3.1. Colorants stability at 4 storage conditions

3.1.1. Color

Color parameters L^* , a^* and b^* were measured in order to analyze the color stability (lightness (L^* 0/100 black/white), greenness ($-a^*$), redness ($+a^*$), blueness ($-b^*$) and yellowness ($+b^*$)) of colorants as a function of storage condition and time. As can be seen in **Figure 1**, at 0 day of storage, colorants presented L^* , a^* and b^* values of 82.4 ± 1.5 , -8.6 ± 0.1 , 40.2 ± 0.8 (E-100);

53.6 ± 1.5, 45.0 ± 1.1, -8.7 ± 0.6 (E-162); and 54.7 ± 2.3, 38.4 ± 1.2, 1.6 ± 0.1 (E-163). These values indicated that the E-100 solution was lighter and yellower, while E-162 and E-163 were redder. Therefore, b* and a* could be considered as determinant parameters to analyze the color stability of E-100 and E-162/E-163, respectively. As shown in **Figure 1**, color stability was dependent on the colorant, storage condition (light and temperature) and time.

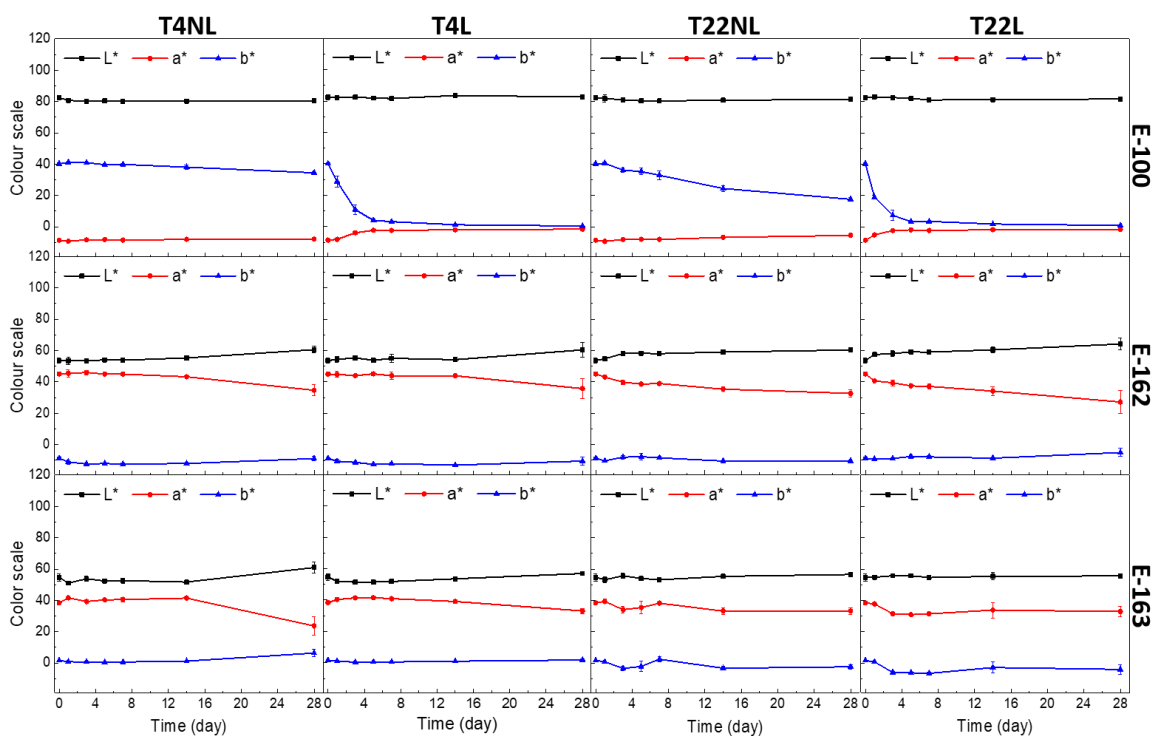


Figure 1. L*, a* and b* color parameters of E-100, E-162 and E-163 colorant solutions (absorbance 1) as a function of storage conditions (T4NL: 4 °C in the dark; T4L: 4 °C in cycles of light-darkness; T22NL: 22 °C in the dark; and T22L: 22 °C in cycles of light-darkness) and time. (n=3)

Regarding the E-100 samples, their color remained largely stable under T4NL storage conditions during storage. However, with a higher storage temperature (T22NL) the b* values were lowered by half, and significant reductions were observed when the samples were exposed to light. In fact, when E-100 samples were illuminated, b* almost decreased to zero. This color loss could be related to photo- and thermal-degradations of curcumin in aqueous solution, as

reported in the literature (Giménez et al., 2015; Hudson et al., 2018). As for E-162, the color remained stable under T4NL storage conditions, although a small color fading could be observed during the last days of storage. With this colorant, the a^* values decreased more quickly with an increase of storage temperature, regardless of the presence of light. This could be related to a thermal degradation process in betanin solutions stored at higher temperatures, as previously reported (Khan, 2016). The decrease in redness (increase in greenness) could in turn cause the increase in lightness observed by the increment of L^* values. Regarding E-163, it behaved similarly to E-162. The small differences can be related to a lower susceptibility of betanins to hydrolytic cleavage than the anthocyanins (Azeredo, 2009). Generally, the differences in color stability between the colorants can be associated with the main coloring compound's chemical structure (Rodriguez-Amaya, 2019).

3.1.2. Color intensity

The stability of colorants can also be visualized by analyzing the changes in their visible absorption spectra during storage (Gérard et al., 2019), and so, the wavelengths that corresponded to the highest absorption (λ_{\max}) and their absorbance (A_{\max}) values are presented in **Table 1** and **Table 2**. E-100, E-162 and E-163 colorants presented λ_{\max} and A_{\max} values of 424 nm & 1.1 ± 0.0 ; 532 nm & 1.1 ± 0.0 ; and 526 nm & 1.1 ± 0.0 , respectively, at 0 days of storage. These λ_{\max} positions correspond with the yellow, red-purple and red colors observed in E-100, E-162 and E-163 solutions, respectively, (Zumdahl & De Coste, 2013) while the A_{\max} values indicated that all samples had the same color intensity. However, these values varied based on the colorant, storage condition and time.

The absorbance values of E-100 barely changed under the T4NL storage conditions. However, an increase in temperature (T22NL) affected the light absorption capacity of E-100 samples and an A_{\max} reduction (hypochromic effect, less color intensity) of 18% was observed after 3 days of storage. In the presence of light, 44% and 67% A_{\max} reductions were observed after 1 day of

storage in T4L and T22L, respectively, showing a faster color intensity reduction at a higher storage temperature. However, the lighting not only had a hypochromic effect on E-100 samples but also a hypsochromic shift (shift of λ_{\max} towards shorter wavelengths). In fact, the presence of light resulted in a noteworthy hypsochromic shift of about 67 nm in samples stored at T4L and T22L after 14 and 7 days of storage, respectively, showing that the color faded at a higher temperature (T22L), related to a destabilization of the curcumin molecule (Moussa et al., 2016). The E-100 was thus, photo-sensitive, and almost completely lost its initial color when exposed to light. This photosensitivity could considerably compromise the pH indicator ability of E-100, which might limit its applications for intelligent packaging development. Encapsulation of E-100 can be a successful strategy to improve stability, as shown in the literature (Gómez-Estaca, Gavara, Hernández-Muñoz, 2015)

Regarding E-162 samples, A_{\max} reductions of about 25% were observed with storage at T4NL and T4L after 28 days, indicating that light had only a slightly accelerating effect on the change in E-162 color stability. However, the increase in temperature had a more significant hypochromic effect, and A_{\max} reductions of 33% were observed in samples stored at T22NL and T22L for 28 days. In these last samples, the increase in temperature along with the presence of light caused a weakened hypsochromic shift of about 5 nm for samples stored at T22L. These results confirmed that E-162 was a thermosensitive colorant. The E-163 colorant samples showed A_{\max} reductions of about 30% after 28 days, irrespective of storage conditions. However, a higher temperature and presence of light induced a slight bathochromic shift (shift of λ_{\max} towards longer wavelengths) of about 3 nm. This thermosensitivity indicated that E-162 and E-163 colorants preserved their color more effectively at lower temperature storage conditions. Thus, color fading might be prevented at lower temperatures and thus, the stability of the colorants will be maintain for their role as pH-indicators.

1 **Table 1.** λ_{\max} and their absorbance (A_{\max}) values of E-100, E-162 and E-163 colorant solutions (absorbance 1) stored at T4NL (4 °C in the dark) and T4L (4 °C
2 in cycles of light-darkness) as a function of time. Two means followed by the same letter in the same row are not significantly ($P > 0.05$) different through
3 the Tukey's multiple range test. (n=3)

| T4NL | | | | | | | | |
|---------------|-----------------------|--------------------------|---------------------------|---------------------------|--------------------------|---------------------------|---------------------------|---------------------------|
| Sample | | 0 day | 1 day | 3 day | 5 day | 7 day | 14 day | 28 day |
| E-100 | λ_{\max} (nm) | 424.0 ± 0.0 ^a | 423.3 ± 0.6 ^a | 423.0 ± 0.0 ^a | 424.0 ± 0.0 ^a | 423.0 ± 0.0 ^a | 423.7 ± 0.6 ^a | 423.3 ± 0.6 ^a |
| | A_{\max} (a.u.) | 1.1 ± 0.0 ^{ab} | 1.1 ± 0.0 ^{ab} | 1.1 ± 0.0 ^{ab} | 1.2 ± 0.0 ^a | 1.0 ± 0.1 ^{ab} | 1.0 ± 0.1 ^{bc} | 0.9 ± 0.0 ^c |
| E-162 | λ_{\max} (nm) | 532.0 ± 0.0 ^a | 532.7 ± 0.6 ^{ab} | 533.0 ± 0.0 ^a | 533.3 ± 0.6 ^a | 532.7 ± 0.6 ^{ab} | 533.0 ± 0.0 ^{ab} | 532.3 ± 1.2 ^{ab} |
| | A_{\max} (a.u.) | 1.1 ± 0.0 ^a | 1.0 ± 0.0 ^a | 1.2 ± 0.0 ^a | 1.2 ± 0.0 ^a | 1.0 ± 0.0 ^a | 0.9 ± 0.1 ^a | 0.8 ± 0.2 |
| E-163 | λ_{\max} (nm) | 526.0 ± 0.0 ^a | 525.3 ± 0.6 ^{ab} | 525.7 ± 0.6 ^{ab} | 526.0 ± 1.0 ^a | 526.0 ± 1.0 ^a | 525.7 ± 0.6 ^{ab} | 522.7 ± 2.3 ^b |
| | A_{\max} (a.u.) | 1.1 ± 0.0 ^{ab} | 1.1 ± 0.0 ^a | 1.2 ± 0.0 ^b | 1.2 ± 0.0 ^{ab} | 1.1 ± 0.0 ^a | 1.1 ± 0.0 ^a | 0.8 ± 0.1 ^c |

| T4L | | | | | | | | |
|---------------|-----------------------|--------------------------|--------------------------|--------------------------|---------------------------|---------------------------|--------------------------|--------------------------|
| Sample | | 0 day | 1 day | 3 day | 5 day | 7 day | 14 day | 28 day |
| E-100 | λ_{\max} (nm) | 424.0 ± 0.0 ^a | 421.0 ± 1.0 ^a | 371.3 ± 6.8 ^b | 363.3 ± 1.2 ^{bc} | 360.7 ± 2.1 ^{cd} | 355.0 ± 4.4 ^d | - |
| | A_{\max} (a.u.) | 1.1 ± 0.0 ^a | 0.6 ± 0.1 ^b | 0.4 ± 0.0 ^c | 0.3 ± 0.1 ^{cd} | 0.2 ± 0.0 ^d | 0.2 ± 0.0 ^d | - |
| E-162 | λ_{\max} (nm) | 532.0 ± 0.0 ^a | 532.0 ± 0.0 ^a | 533.0 ± 1.0 ^a | 533.0 ± 0.0 ^a | 533.0 ± 0.0 ^a | 533.0 ± 1.0 ^a | 531.7 ± 2.3 ^a |
| | A_{\max} (a.u.) | 1.1 ± 0.0 ^a | 1.0 ± 0.0 ^b | 1.2 ± 0.1 ^a | 1.1 ± 0.0 ^a | 1.0 ± 0.0 ^b | 1.0 ± 0.0 ^b | 0.9 ± 0.0 ^c |
| E-163 | λ_{\max} (nm) | 526.0 ± 0.0 ^a | 525.7 ± 0.6 ^a | 525.7 ± 0.6 ^a | 526.0 ± 0.0 ^a | 526.0 ± 0.0 ^a | 526.0 ± 0.0 ^a | 525.3 ± 0.6 ^a |
| | A_{\max} (a.u.) | 1.1 ± 0.0 ^{abc} | 1.1 ± 0.0 ^{cd} | 1.2 ± 0.1 ^{ab} | 1.2 ± 0.0 ^a | 1.1 ± 0.0 ^{bcd} | 1.0 ± 0.0 ^d | 0.8 ± 0.0 ^e |

4

5 **Table 2.** λ_{\max} and their absorbance (A_{\max}) values of E-100, E-162 and E-163 colorant solutions (absorbance 1) stored at T22NL (22 °C in the dark) and T22L
6 (22 °C in cycles of light-darkness) as a function of time. Two means followed by the same letter in the same row are not significantly ($P > 0.05$) different
7 through the Tukey's multiple range test. (n=3)

| T22NL | | | | | | | | |
|---------------|-----------------------|--------------------------|---------------------------|---------------------------|--------------------------|---------------------------|---------------------------|---------------------------|
| Sample | | 0 day | 1 day | 3 day | 5 day | 7 day | 14 day | 28 day |
| E-100 | λ_{\max} (nm) | 424.0 ± 0.0 ^a | 424.0 ± 0.0 ^a | 424.0 ± 0.0 ^a | 424.0 ± 0.0 ^a | 424.3 ± 0.6 ^a | 424.0 ± 0.0 ^a | 423.7 ± 0.6 ^a |
| | A_{\max} (a.u.) | 1.1 ± 0.0 ^a | 1.1 ± 0.0 ^{ab} | 0.9 ± 0.1 ^{ab} | 1.0 ± 0.0 ^{ab} | 0.9 ± 0.2 ^b | 0.5 ± 0.1 ^c | 0.4 ± 0.0 ^c |
| E-162 | λ_{\max} (nm) | 532.0 ± 0.0 ^a | 532.7 ± 0.6 ^a | 532.0 ± 0.0 ^a | 532.7 ± 0.6 ^a | 531.7 ± 0.6 ^a | 533.0 ± 1.0 ^a | 533.3 ± 2.1 ^a |
| | A_{\max} (a.u.) | 1.1 ± 0.0 ^a | 1.0 ± 0.0 ^{ab} | 1.0 ± 0.1 ^{ab} | 0.9 ± 0.1 ^b | 0.9 ± 0.1 ^b | 0.9 ± 0.1 ^{bc} | 0.7 ± 0.1 ^c |
| E-163 | λ_{\max} (nm) | 526.0 ± 0.0 ^a | 526.0 ± 0.0 ^a | 529.0 ± 1.0 ^a | 528.3 ± 3.2 ^a | 525.0 ± 1.0 ^a | 529.0 ± 1.0 ^a | 528.7 ± 2.1 ^a |
| | A_{\max} (a.u.) | 1.1 ± 0.0 ^a | 1.1 ± 0.0 ^{ab} | 1.0 ± 0.2 ^{ab} | 1.0 ± 0.1 ^{ab} | 1.1 ± 0.0 ^{ab} | 1.0 ± 0.1 ^{ab} | 0.9 ± 0.0 ^b |
| T22L | | | | | | | | |
| Sample | | 0 day | 1 day | 3 day | 5 day | 7 day | 14 day | 28 day |
| E-100 | λ_{\max} (nm) | 424.0 ± 0.0 ^a | 406.0 ± 10.4 ^b | 359.0 ± 1.7 ^c | 355.3 ± 1.2 ^c | 357.0 ± 4.6 ^c | - | - |
| | A_{\max} (a.u.) | 1.1 ± 0.0 ^a | 0.4 ± 0.0 ^b | 0.3 ± 0.0 ^{bc} | 0.2 ± 0.0 ^c | 0.3 ± 0.1 ^c | - | - |
| E-162 | λ_{\max} (nm) | 532.0 ± 0.0 ^a | 532.7 ± 0.6 ^a | 532.7 ± 0.6 ^a | 532.7 ± 0.6 ^a | 532.0 ± 0.0 ^a | 532.0 ± 1.0 ^a | 527.3 ± 0.6 ^b |
| | A_{\max} (a.u.) | 1.1 ± 0.0 ^a | 1.00 ± 0.0 ^{ab} | 1.0 ± 0.0 ^{ab} | 1.0 ± 0.1 ^{bc} | 0.9 ± 0.1 ^{bc} | 0.9 ± 0.1 ^{bc} | 0.8 ± 0.0 ^c |
| E-163 | λ_{\max} (nm) | 526.0 ± 0.0 ^a | 525.7 ± 0.6 ^a | 530.0 ± 1.0 ^{ab} | 532.0 ± 1.0 ^b | 531.0 ± 1.0 ^{ab} | 529.7 ± 4.0 ^{ab} | 529.7 ± 2.5 ^{ab} |
| | A_{\max} (a.u.) | 1.1 ± 0.0 ^a | 1.1 ± 0.0 ^{ab} | 0.9 ± 0.1 ^{bc} | 0.9 ± 0.0 ^{bc} | 0.8 ± 0.0 ^c | 1.0 ± 0.2 ^{abc} | 0.9 ± 0.1 ^{bc} |

8

3.1.3. Thermal stability

In order to further analyze the effect of temperature in colorants stability, the thermal stability measurements of colorants was investigated. As shown in **Figure 2 I** and **II**, E-100, E-162 and E-163 presented different behaviors with diverse weight loss stages in presence of thermo-oxidative reactions. E-100 presented an initial weight loss (3.5%) at 245 °C and a large weight loss (63.9%) at 408 °C. E-162 showed 6.7% weight loss at lower temperatures (140 °C) and above this temperature a significant rapid degradation occurred with increasing temperature (213 °C, 31.9%). E-163 behaved similar to E-162 since 5.8 % weight was lost at 134 °C and its quick degradation continued with the increase in temperature (210 °C, 29.3%). Therefore, these results confirmed that E-162 and E-163 colorants were more susceptible to thermal-degradation than E-100, as shown in the assessment of color stability.

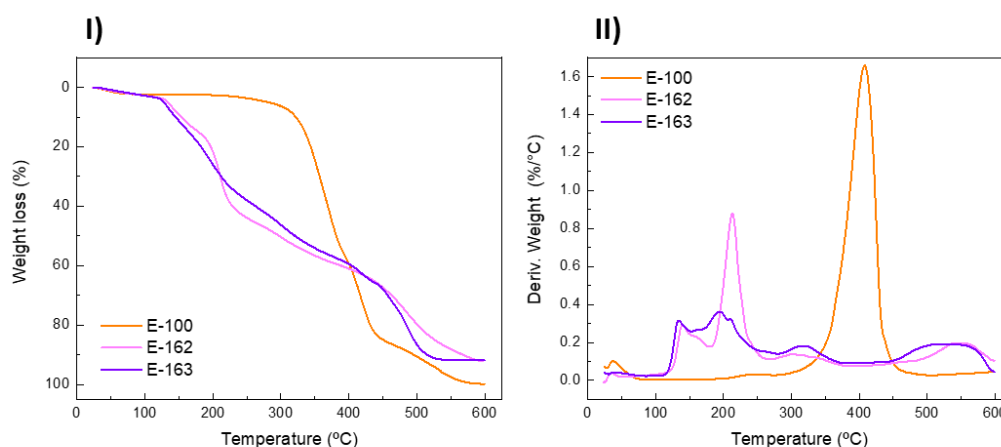


Figure 2. I) TGA and and II) TGA derivative (deriv.) results of freeze-dried E-100, E-162 and E-163 colourant under air atmosphere conditions.

Regarding packaging production processes, different manufacturing methods (solution casting, compression molding, freeze-drying combined with indirect 3D printing, electrospinning, extrusion and injection) can be used to prepare food packaging products (films, foam trays, mats) (Etxabide et al., 2018). In these processes different temperatures are used, which can compromise the color properties of colorants (Table 3), especially of E-162 and E-163 when used

as additives. In fact, any processing requiring temperatures above 130 °C (especially in polyolefin-based packaging manufacturing) might compromise the stability of E-162 and E-163 colorants while temperatures above 250 °C could affect the integrity of E-100 colorant. Therefore, considerable attention should be paid to manufacturing parameters when these colorants are used for intelligent packaging development.

Table 3. Examples of materials, manufacturing methods and process temperatures (T) used in food packaging development, and possible weight loss of studied colorants at these processing temperatures.

| Packaging material | Manufacturing method | T (°C) | Weight loss (%) E-100/E-162/E-163 | Reference |
|----------------------------|----------------------|--------|-----------------------------------|-----------------------|
| Starch | Compression molding | 120 | 2.3 / 3.5 / 3.7 | Ceballos et al, 2020 |
| Soy protein | | 150 | 2.4 / 9.2 / 11.3 | Ciannamea et al, 2016 |
| Polyethylene | Twin-screw extruder | 180 | 2.5 / 15.2 / 19.2 | Jo et al., 2018 |
| Polypropylene | | 200 | 2.6 / 21.8 / 26.1 | |
| Polyethylene terephthalate | | 255 | 3.8 / 44.6 / 38.8 | Li et al., 2019 |

3.1.4. pH and turbidity

The stability of the colorants was further analyzed using pH and turbidity assessments. The initial pHs of E-100, E-162 and E-163 solutions were 6.7 ± 0.2 , 5.0 ± 0.0 and 3.7 ± 0.0 , respectively (**Figure 3-I**). These results indicated that the colorants solutions presented neutral (E-100) and acidic (E-162 and E-163) behaviors, due to the presence of citric acid in the latter two colorant formulations. However, the pH of colorants changed as a function of storage condition and time, as did the turbidity (**Figure 3-II**). E-100 samples presented almost no pH and turbidity alterations, irrespective of storage conditions and time, while in E-162 samples a decrease in pH and an increase in turbidity were observed. These alterations were accelerated at high temperatures (T22), irrespective of lighting. As for E-163, these samples presented an increase in pH and turbidity, mainly under high temperature storage conditions. These pH and turbidity variations

could be related to the presence of microorganisms in the samples, since through their metabolic activity microorganisms can produce acidic or alkaline metabolites that change the pH and the clarity of the medium, and more quickly at a higher storage temperature (da Silva et al., 2019; Ratzke & Gor, 2018; Ziegler et al., 2019). Therefore, the potential microbial growth was assessed using a turbidimeter and the results are shown in **Figure 3-II**.

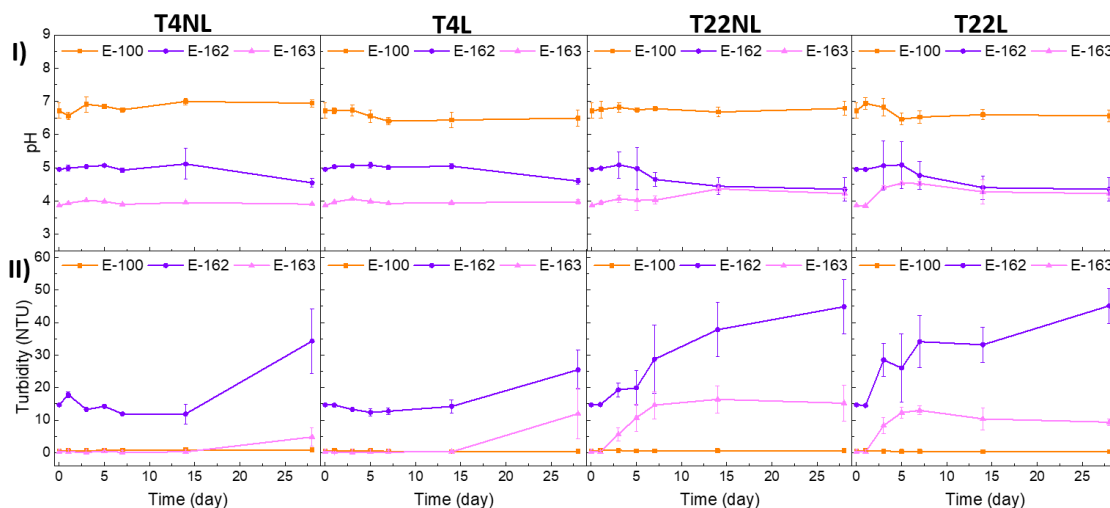


Figure 3. I) pH and II) turbidity values of E-100, E-162 and E-163 colorant solutions (absorbance 1) as a function of storage conditions (T4NL: 4 °C in the dark; T4L: 4 °C in cycles of light-darkness; T22NL: 22 °C in the dark; and T22L: 22 °C in cycles of light-darkness) and time. (n=3)

E-100 samples presented almost no turbidity alterations, irrespective of storage conditions and time, which was related to the small pH variations in the samples. However, turbidity of E-162 and E-163 samples significantly increased after 14 and 3 days of storage at 4 and 22 °C, respectively, regardless of lighting. Considering that generally microorganisms prefer a neutral pH for optimum growth and that acidity inhibits most microbial growth, these results showed a possible antimicrobial property of the E-100 colorant. This could be related to both, the main coloring compound (curcumin) extracted from *Curcuma longa*, which has been shown to inhibit bacterial activity in solution (Liu et al., 2016; Wang et al., 2017) and the emulsifier included in the E-100 colorant (Nielsen et al., 2016). However, the low amount of E-100, could also be a factor in the lack of bacterial growth, given that low nutrient concentrations would be present

in the samples (Shehata & Marr, 1971). As for betanin and anthocyanin extracted from red beet and black carrots, respectively, their antimicrobial properties have been demonstrated (Koosha & Hamed, 2019; Kumar & Brooks, 2018), as has the citric acid additive (Uranga et al., 2019). However, in our study, the colorants amounts used in the samples did not inhibit microbial growth in the E-162 and E-163 samples, and it would be due to a bigger presence of nutrients, mainly sugars, (Ersus & Yurdagel, 2007; Wruss et al., 2015) in these samples.

In order to better understand the reason for the lack of turbidity in the E-100 samples, minimum bactericidal concentration (MBC) measurements were conducted in concentration ranges greater and lower than concentrations (absorbance 1) used in this study, and against two pathogenic bacteria, Gram-positive *S. aureus* and Gram-negative *E. coli*. As shown in **Figure 4**, the colorants did not exert an antimicrobial effect over any analyzed concentration and against either bacterial strain tested, since confluent colony growths were observed in all samples and concentrations. Therefore, the lack of turbidity in E-100 samples could be mainly related to a low nutrient content (no sugars, mainly fat) in the samples.

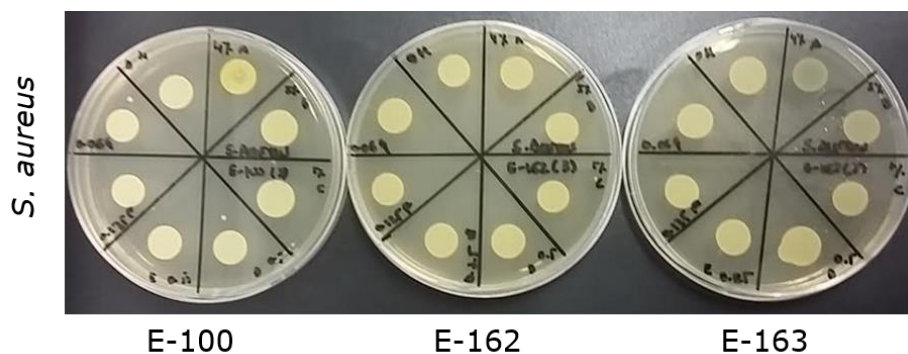


Figure 4. Minimum bactericidal concentration (MBC) measurements of E-100, E-162 and E-163 colourants against *S. aureus*. (n=3)

Considering these results, the use of colorants as additives of the packaging material such as films would improve the pH stability of colorants, especially of E-162 and E-163, due to the low amounts of water in the packing material. This can be obtained by adding the colorants into

packaging formulations and preparing solid packages that can be in constant contact (trays and cling films) or in non-contact (peelable lidding film used in trays) with food.

3.2. Effect of concentration and pH on color change

The food colorants used in this study are established pH-indicators (Musso et al., 2017; Qin et al., 2020), since their colors change when the pH varies (**Figure 5-I** and **Figure 5-III**). These color variations are related to molecular structural transformations which are dependent on the pH and induce λ_{\max} shifts, since each colored product absorbs light at specific wavelengths (Kennedy & Waterhouse, 2000; Zumdahl & De Coste, 2013). However, in order to obtain a good visual color variability or clear color response to pH variations, colorant concentrations must be taken into account (Pourjavaher et al., 2017). Therefore, solutions with different color intensities (absorbances of 0.25, 0.50 and 1.00, **Figure 5-II**) were studied in order to assess the colorant concentration effect on color variability as a function of pH. The pH of the solutions were modified by adding different molarities of acid and basic solutions, and the color was analyzed using DigiEye (**Figure 5-III**) and UV-vis spectrophotometer (**Figure 6**).

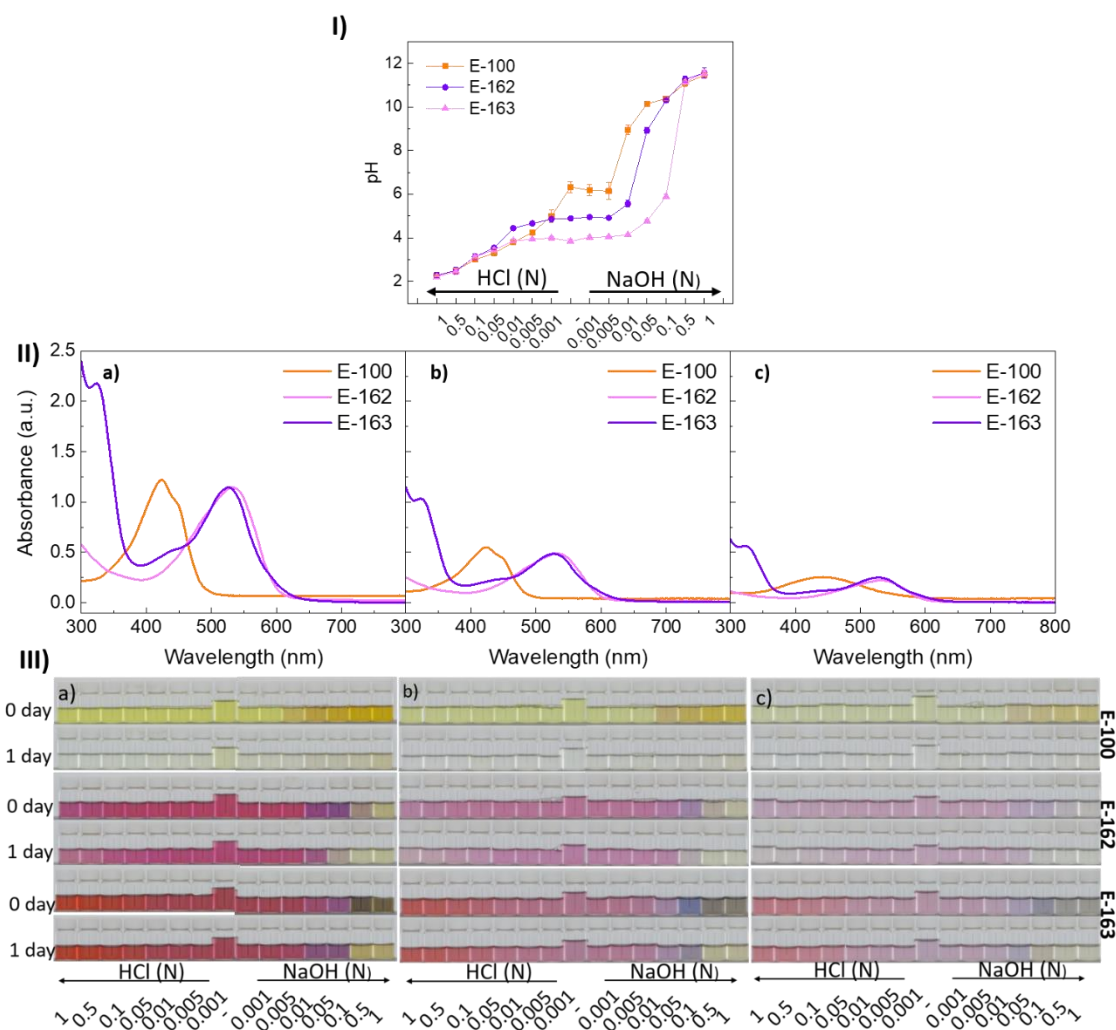


Figure 5. I) pH values of E-100, E-162 and E-163 colorant solutions after pH modification; **II)** Colour intensities of E-100, E-162 and E-163 colourant solutions with absorbance a) 1.00, b) 0.50 and c) 0.25; **III)** Color variation of E-100, E-162 and E-163 colorant solutions as a function of pH, storage (0 and 1 day in T22L (22 °C in cycles of light-darkness)) and solution color intensity: absorbance a) 1.00, b) 0.50 and c) 0.25. (n=3)

As expected, the color intensity of the solutions decreased as the colorant concentration was lowered, as observed in **Figure 5-II** and **Figure 5-III**. Additionally, pH modification induced color changes that were concentration and colorant dependent. An increase in pH (pH >9) resulted in color changes from yellow to brown-yellow ($L^* \downarrow$, $+a^* \uparrow$, $+b^* \uparrow$) in E-100 samples, irrespective of colorant concentration. This color change was also seen in a bathochromic shift to 465 nm in

the visible spectra (**Figure 6**) and was related to the deprotonation of curcumin under alkaline condition, as previously observed by Liu et al., 2018 and Chen et al., 2020. In fact, the keto form of curcumin dominates in acidic and neutral media while in basic media the enol form predominates. However, all samples lost their color ($L^* =$, $-a^* \downarrow$, $+b^* \downarrow$) after storage (T22L, 1 day), in particular the samples at the lowest concentrations (absorbance 0.25). This color fading was also seen through a hypsochromic shift to 367 nm (observed color: yellow) and hypochromic effect (intensity reduction), leading to colorless solutions due to the degradation of the main coloring compound (curcumin).

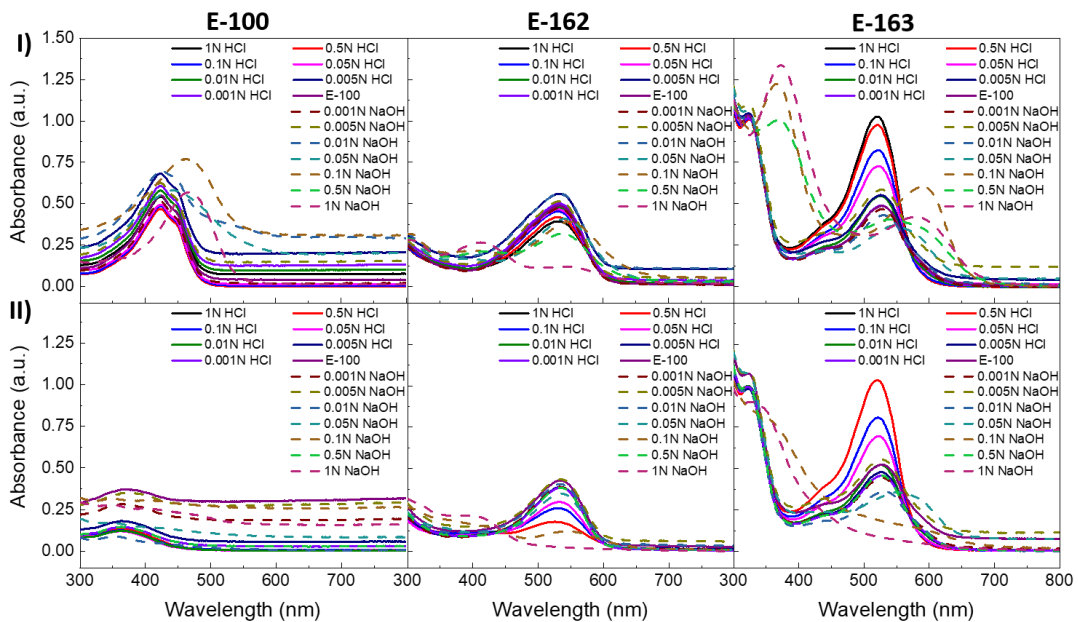


Figure 6. Color intensities of E-100, E-162 and E-163 colorant solutions (absorbance 0.5) as a function of pH and storage at T22L (22 °C in cycles of light-darkness) for: **I)** 0 and **II)** 1 day. (n=3)

Regarding E-162 samples, pH modification induced color changes from red-purple to both rosy and violet when the solution pH was decreased ($\text{pH} < 2$, anionic form, $L^* =$, $+a^* \downarrow$, $-b^* \uparrow$) and increased ($\text{pH} > 9$, mono-, di-, and tri-deprotonated forms, $L^* =$, $+a^* \downarrow$, $-b^* \uparrow$), respectively (Slimen, Najjar, Abderrabba, 2017). A higher alkalisation ($\text{pH} > 11$) turned the red-purple solutions into light yellow ($L^* \uparrow$, $+a^* \downarrow$, $+b^* \uparrow$), which points to a betanin degradation. A pH decrease led to a hypochromic effect in E-162 samples which was shown in as a lower color

intensity (observed color: rosy). An increase in pH, however, not only had a hypochromic effect, but also presented a small bathochromic shift up to 550 nm (observed color: violet). However, stronger alkalinisation of the colorant presented a new absorbance band with λ_{\max} at 415 nm (observed color: yellow), while the initial λ_{\max} (532 nm) band disappeared, which corresponded with color loss due to betanin molecule destabilization. It is worth mentioning that better color responses were observed at higher colorant concentrations. After storage, acidified (pH <2) and alkalified (pH >10) samples showed color fading ($L^* \uparrow$, $+a^* \downarrow$, $-b^* \downarrow$ and $L^* \uparrow$, $-a^* \uparrow$, $+b^* =$) while the samples stored at pH ≥ 3 and pH ≤ 9 largely maintained their color intensities, irrespective of initial coloring concentrations. Similar pH-stability behaviors were reported in the literature (Slimen, Najar, Abderrabba, 2017). These results indicated that E-162 exhibited a clearer color response at higher colorant concentrations and that it was more stable under moderate pH conditions.

When pH was modified in E-163 samples, the color changed from reddish to both stronger reddish and purple when pHs decreased (pH <3.5, flavylium cation, $L^* =$, $+a^* \uparrow$, $+b^* \uparrow$) and increased (pH >6, quinonoidal form, $L^* \downarrow$, $+a^* \downarrow$, $-b^* \uparrow$), respectively. Thus, a pH decrease lead to a hyperchromic effect, which resulted in a higher red color intensity. The increase in pH, nevertheless, had a hypochromic effect as well as a small bathochromic shift up to 590 nm (observed color: violet-blue). However, stronger alkalinisation of the colorant induced the appearance of a new absorbance band with λ_{\max} at 370 nm (observed color: yellow), which could correspond to the yellow carbinol form of anthocyanin. The decrease in colorant concentration (intensities 0.5 and 0.25) resulted in a better visual color variability, since redder (flavylium cation form of anthocyanin, $L^* =$, $+a^* \uparrow$, $+b^* \uparrow$) and blue (blue quinonoidal form of anthocyanin, $L^* =$, $+a^* \downarrow$, $-b^* \uparrow$) colors were observed in solutions with pH <3.5 and pH 10-11, respectively. In addition to that, dark green colors were also seen when the pH was greater than 11 ($L^* =$, $-a^* \uparrow$, $+b^* \uparrow$). After storage, the alkalified (pH >10) samples showed a color loss (hypochromic effect, $L^* \uparrow$, $+a^* \downarrow$, $+b^* \uparrow$), which indicated a destabilization of the anthocyanin

molecule (Kennedy & Waterhouse, 2000). Similar results were found in literature (Tang et al., 2019). The results of this study indicated that E-163 exhibited a clearer color response at lower colorant concentrations and that it was more stable under acidic and moderate basic conditions.

In view of color variation responses of the colorants under basic conditions, E-100, E-162 and E-163 could be used to control freshness in fish and meat products, for instance salmon and chicken, due to manner in which these foodstuff release chemicals such as volatile amines during spoilage. However, in an acidic medium, E-162 and E-163 colorants could be applied to monitor ready-to-eat vegetable food products (Yousefi et al., 2019).

3.3. Color reversibility

The color reversibility of colorants was also analyzed in order to observe the color change capacity of each colorant in response to extreme pH stimulus and storage conditions (**Figure 7**). All colorants presented color variations to quick and strong acidified and alkalified modification as the color continued varying over time, irrespective of colorant concentration (data not shown). These changes were due to the reversible structural transformation of the main coloring compounds, such as from enol form (brown-yellow) to keto form (yellow) when basic environments turned into acidic in curcumin containing solutions. Another reversible transformation would be from flavylum cation form (red) to quinonoidal form (blue) when moving from acidic to basic environments with anthocyanin containing solutions (Chen et al., 2020). However, as expected, the samples lost their ability to reverse their color with further pH modifications once the main coloring compounds were degraded.

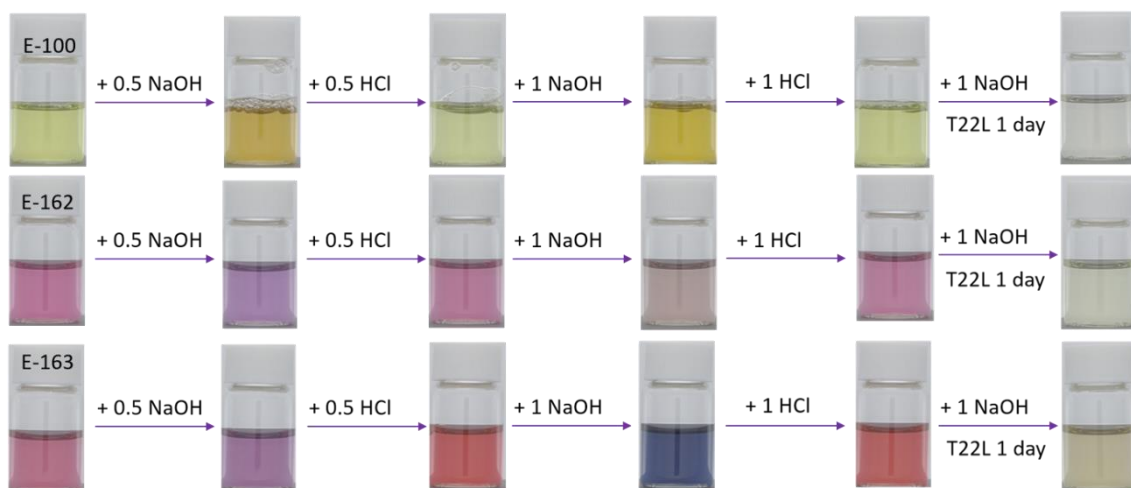


Figure 7. Colour reversibility in E-100, E-162 and E-163 colourant solutions of 0.5 absorbance.

4. CONCLUSIONS

In this study, the color stability and variability of curcumin (E-100), betanin (E-162), and anthocyanin (E-103) containing natural food colorant solutions under different commercial food storage conditions and pHs were examined. E-100 was a more powerful colorant but lost its pH-indicator ability, while E-162 and E-163, retained their initial color intensities for 28 days due to their better stability under light exposure. However, they were prone to degrade at higher temperatures. E-163 exhibited better color variations and stability to a wider range of pHs before and after storage, showing greater potential for the development of intelligent packaging for monitoring the quality of chilled food. Consequently, this research has shown that betanin and anthocyanin containing food colorants are appropriated for the development of intelligent food packaging systems. These colorants should be used as additives within packaging formulation and manufactured in low temperature processes in order to not compromise their color properties and prolong their stability and pH-indicator ability.

ACKNOWLEDGEMENT

A.E. thanks the Ministry of Science, Innovation and Universities (Juan de la Cierva contract).

REFERENCES

Azeredo, H. M. C. (2009). Betalains: properties, sources, applications, and stability – a review. *International Journal of Food Science and Technology*, *44*, 2365-2376.

Ceballos, R. L. Ochoa-Yepes, O., Goyanes, S., Bernal, C., Famá L. (2020). Effect of yerba mate extract on the performance of starch films obtained by extrusion and compression molding as active and smart packaging. *Carbohydrate Polymers*, *244*, 116495.

Ciannamea, E. M., Stefani, P.M., Ruseckaite, R. A. (2016). Properties and antioxidant activity of soy protein concentrate films incorporated with red grape extract processed by casting and compression molding. *LWT*, *74*, 353-362.

Chen, H. Z., Zhang, M., Bhandari, B., & Yang, C. H. (2020). Novel pH-sensitive films containing curcumin and anthocyanins to monitor fish freshness. *Food Hydrocolloids*, *100*, 105438.

Commission Regulation (EU) No 1129/2011 of 11 November 2011 amending Annex II to Regulation (EC) No 1333/2008 of the European Parliament and of the Council by establishing a Union list of food additives.

da Silva, N. B., Carciofi, B. A. M., Ellouze, M., & Baranyi, J. (2019). Optimization of turbidity experiments to estimate the probability of growth for individual bacterial cells. *Food Microbiology*, *83*, 109-112.

Ersus S., & Yurdagel U. (2007). Microencapsulation of anthocyanin pigments of black carrot (*Daucus carota* L.) by spray drier. *Journal of Food Engineering*, *80*, 805-12.

Etxabide, A., Garrido, T., Uranga, J., Guerrero, P., & de la Caba, K. (2018). Extraction and incorporation of bioactives into protein formulations for food and biomedical applications. *International Journal of Biological Macromolecules*, *120*, 2094–2105.

European Commission, 2009. EU guidance to the commission regulation on active and intelligent materials and articles intended to come into contact with food.

European Commission, 2018. Date marking and food waste.

https://ec.europa.eu/food/safety/food_waste/eu_actions/date_marking_en

Fang Z., Zhao Y., Warner R.D., & Johnson S. K. (2017). Active and intelligent packaging in meat industry. *Trends in Food Science and Technology*, 61, 60-71.

FAO, 2015. Global Initiative on Food Loss and Waste Reduction. Global Initiative on Food Loss and Waste Reduction.

FDA. U.S. Food and Drug Administration, 2019. Confused by Date Labels on Packaged Foods?

<https://www.fda.gov/consumers/consumer-updates/confused-date-labels-packaged-foods>

Gérard V., Ay E., Morlet-Savary F., Graff B., Galopin C., Ogren T., Mutilangi, W., & Lalevée, J. (2019). Thermal and photochemical stability of anthocyanins from black carrot, grape juice, and purple sweet potato in model beverages in the presence of ascorbic acid. *Journal of Agricultural and Food Chemistry*, 67, 5647-60.

Giménez, P. J., Fernández-López, J. A., Angosto, J. M., & Obón J. M. (2015). Comparative thermal degradation patterns of natural yellow colorants used in foods. *Plant Foods for Human Nutrition*, 70, 380-387.

Gómez-Estaca, J., Gavara, R., & Hernández-Muñoz, P. (2015). Encapsulation of curcumin in electrosprayed gelatin microspheres enhances its bioaccessibility and widens its uses in food applications. *Innovative Food Science & Emerging Technologies*, 29, 302-307.

Hudson, E. A., de Paula, H. M. C., Ferreira, G. M. D., Ferreira, G. M. D., Hespanhol, M. C. D., da Silva, L. H. M., & Pires A. C. D. S. (2018). Thermodynamic and kinetic analyses of curcumin and bovine serum albumin binding. *Food Chemistry*, 242, 505-512.

Jo, Y., Garcia, C. V., Ko, S., Lee, W., Shin, G. H., Choi, J. C., Park, S. J., Kim, J. T. (2018). Characterization and antibacterial properties of nanosilver-applied polyethylene and polypropylene composite films for food packaging applications. *Food Bioscience*, 23, 83-90.

Kang S., Wang H., Guo M., Zhang L., Chen M., Jiang S., Li, X., & Jiang, S. (2018). Ethylene-vinyl alcohol copolymer–montmorillonite multilayer barrier film coated with mulberry anthocyanin for freshness monitoring. *Journal of Agricultural and Food Chemistry*, *66*, 13268-76.

Kennedy, J. A., & Waterhouse, A. L. (2000). Analysis of pigmented high-molecular-mass grape phenolics using ion-pair, normal-phase high-performance liquid chromatography. *Journal of Chromatography A*, *866*, 25-34.

Khan, M.I. (2016). Stabilization of betalains: A review. *Food Chemistry*, *197*, 1280-1285.

Koosha, M., & Hamed, S. (2019). Intelligent Chitosan/PVA nanocomposite films containing black carrot anthocyanin and bentonite nanoclays with improved mechanical, thermal and antibacterial properties. *Progress in Organic Coatings*, *127*, 338-347.

Kumar, S., & Brooks, M.S.L. (2018). Use of red beet (*Beta vulgaris* L.) for antimicrobial applications—a critical review. *Food and Bioprocess Technology*, *11*, 17-42.

Li, B., Wang, Z. W., Bai, Y. H. (2019). Determination of the partition and diffusion coefficients of five chemical additives from polyethylene terephthalate material in contact with food simulants. *Food Packaging and Shelf Life*, *21*, 100332.

Liu, Y., Cai, Y., Jiang, X., Wu, J., & Le, X. (2016). Molecular interactions, characterization and antimicrobial activity of curcumin–chitosan blend films. *Food Hydrocolloids*, *52*, 564-572.

Liu, J., Wang, H., Wang, P., Guo, M., Jian, S., Li, X., Jiang, S. (2018). Films based on κ -carrageenan incorporated with curcumin for freshness monitoring. *Food Hydrocolloids*, *83*, 134-142.

Moussa, Z., Hmadeh, M., Abiad, M. G., Dib, O. H., & Patra, D. (2016). Encapsulation of curcumin in cyclodextrin-metal organic frameworks: Dissociation of loaded CD-MOFs enhances stability of curcumin. *Food Chemistry*, *212*, 485-494.

Musso, Y. S., Salgado, P. R., & Mauri, A. N. (2017). Smart edible films based on gelatin and curcumin. *Food Hydrocolloids*, *66*, 8-15.

Nielsen, C. K., Kjems, J., Mygind, T., Snabe, T., & Meyer, R. L. (2016). Effects of Tween 80 on growth and biofilm formation in laboratory media. *Frontiers Microbiology*, *7*, 1878.

Pourjavaher, S., Almasi, H., Meshkini, S., Pirsá, S., & Parandi, E. (2017). Development of a colorimetric pH indicator based on bacterialcellulose nanofibers and red cabbage (*Brassica oleracea*) extract. *Carbohydrates Polymers*, *156*, 193-201.

Qin, Y., Liu, Y., Zhang, X., & Liu, J. (2020). Development of active and intelligent packaging by incorporating betalains from red pitaya (*Hylocereus polyrhizus*) peel into starch/polyvinyl alcohol films. *Food Hydrocolloids*, *100*, 105410.

Raak, N., Symmank, C., Zahn, S., Aschemann-Witzel, J., & Rohm, H. (2017). Processing- and product-related causes for food waste and implications for the food supply chain. *Waste management*, *61*, 461-472.

Ratzke, C., & Gor, J. (2018). Modifying and reacting to the environmental pH can drive bacterial interactions. *PLOS Biology*, *16*, 2004248.

Rodriguez-Amaya, D. B. (2019). Update on natural food pigments - A mini-review on carotenoids, anthocyanins, and betalains. *Food Research International*, *124*, 200-205.

Shehata, T. E., & Marr, A. (1971). Effect of nutrient concentration on the growth of *Escherichia coli*. *Journal of Bacteriology*, *107*, 210-216.

Slimen, I.B., Najar, T., & Abderrabba, M. (2017). Chemical and Antioxidant Properties of Betalains. *Journal of Agricultural and Food Chemistry*, *65*, 675-689.

- Tang, B., He, Y., Liu, J., Zhang, J., Li, J., Zhou, J., Ye, Y., Wang, J., & Wang, X. (2019). Kinetic investigation into pH-dependent color of anthocyanin and its sensing performance. *Dyes and Pigments*, *170*, 107643.
- Uranga, J., Puertas, A. I., Etxabide, A., Dueñas, M. T., Guerrero, P., & de la Caba. K. (2019). Citric acid-incorporated fish gelatin/chitosan composite films. *Food Hydrocolloids*, *86*, 95-103.
- Wang, H., Hao, L., Wang, P., Chen, M., Jiang, S., & Jiang, S. (2017). Release kinetics and antibacterial activity of curcumin loaded zein fibers. *Food Hydrocolloids*, *63*, 437-446.
- West M. E., & Mauer L. J. (2013). Color and chemical stability of a variety of anthocyanins and ascorbic acid in solution and powder forms. *Journal of Agricultural and Food Chemistry*, *61*, 4169-79
- Wilson, N. L. W, Rickard, B. J., Saputo, R., & Ho, S. T. (2017). Food waste: The role of date labels, package size, and product category. *Food Quality and Preference*, *55*, 35-44.
- Won K., Jang, N. Y., & Jeon J. (2016). A natural component-based oxygen indicator with in-pack activation for intelligent food packaging. *Journal of Agricultural and Food Chemistry*, *64*, 9675-9.
- Wruss, J., Waldenberger, G., Huemer, S., Uygun, P., Lanzerstorfer, P., Müller, U., Höglinger, O., & Weghuber, J. (2015). Compositional characteristics of commercial beetroot products and beetroot juice prepared from seven beetroot varieties grown in Upper Austria. *Journal of Food Composition and Analysis*, *42*, 46-55.
- Yam, K. L. (2012). Intelligent packaging to enhance food safety and quality. In: K. L., Yam, D. S., Lee (Eds.), *Emerging food packaging technologies: Principles and practice*, (pp. 137-174). Philadelphia: Woodhead Publishing Limited.

Yousefi, H., Su, H. M., Imani, S. M., Alkhaldi, K., Filipe, C. D. M., & Didar, T. F. (2019). Intelligent food packaging: A review of smart sensing technologies for monitoring food quality. *ACS Sensors*, *4*, 808–821.

Zhai, X., Li Z., Zhang J., Shi J., Zou X., Huang X., Zhang, D., Sun, Y., Yang, Z., Holmes, M., Gong, Y., & Povey, M. (2018). Natural biomaterial-based edible and pH-sensitive films combined with electrochemical writing for intelligent food packaging, *Journal of Agricultural and Food Chemistry*, *66*, 12836-12846.

Ziegler, M., Kent, D., Stephan, R., & Guldimann, C. (2019). Growth potential of *Listeria monocytogenes* in twelve different types of RTE salads: Impact of food matrix, storage temperature and storage time. *International Journal of Food Microbiology*, *296*, 83-92.

Zumdahl S. S., & De Coste, D. J. (2013). *Chemical Principles* (7th ed). Belmont: Brook/Cole.